Available online at www.sciencedirect.com

ScienceDirect

Ceramics International 40 (2014) 919–927

CERAMICS INTERNATIONAL

www.elsevier.com/locate/ceramint

Polymerization-induced phase separation in the preparation of macroporous TiO_2/SiO_2 thin films

Yue Situ, Tao Huang, Yanfeng Chen, Weixin Huang, Hong Huang*

School of Chemistry and Chemical Engineering, South China University of Technology, Guangzhou 510640, People's Republic of China

Received 13 June 2013; received in revised form 20 June 2013; accepted 24 June 2013
Available online 4 July 2013

Abstract

Macroporous TiO_2/SiO_2 (TS) composite thin films deposited on glass substrates were successfully prepared through a versatile template-free sol–gel approach based on the hydrolysis and polycondensation of tetrabutyl titanate and tetraethyl orthosilicate. A theoretic explanation for the formation of porous morphology was discussed in relation to the polymerization-induced phase separation and the concurrent sol–gel transition. The mechanism of phase separation was attributed to the spinodal decomposition. The field emission scanning electron microscope (FESEM) results indicate that the surface morphologies of TS thin films strongly depend on the amount of SiO_2 sols (mole fraction) and aging time before spin-coating. A systemic method of long-range pore size tailoring for macroporous TS composite thin film was achieved by adjusting mole ratio of TiO_2 to SiO_2 and the aging time.

Keywords: A. Sol–gel process; Macroporous; TiO_2/SiO_2 thin films; Phase separation; Polymerization-induced

1. Introduction

Titanium dioxide (TiO_2) thin films have been one of the most promising multifunctional materials during the last decades, due to their high photoactivity and photoelectrochemical property, strong redox activity as well as outstanding hydrophilicity [1,2]. They show great potential applications in catalysis, water purification, antibacterium, anticorrosion, photovoltaic cells, self-cleaning, antifogging, heat transfer and biomedical applications [3–9]. Recently, special attention has been focused on the surface structural or chemical modifications for TiO_2 thin films to improve their photoelectrochemical or superhydrophilic properties. Microporous structure and surface morphological control of TiO_2 thin films have been demonstrated to be highly beneficial for enhancing their photocatalytic performance and wettability [10–12]. In addition, strengthened photocatalytic effects and superhydrophilic performance have been observed in composite TiO_2 thin films prepared by mixing with SiO_2 or mono-layer coverage/substrate by SiO_2 [13–17].

A variety of synthetic methods have been developed to prepare TiO_2 thin films such as sol–gel method [18], sputtering techniques [19], chemical vapor deposition [20], anodic electrophoretic deposition [21], ultrasonic spray pyrolysis [22], layer-by-layer (LBL) assembly [11], inkjet printing [3] and hydrothermal synthesis [23]. Sol–gel process is one of the most widely used techniques to fabricate porous structures for its attractive advantages, i.e., easy to form uniform multi-component films and control structure with different additives [18]. It has been reported that porous TiO_2 films have been prepared via surface modification with several templates or pre-existing particles including polystyrene (PS) [24], polyethylene glycol (PEG) [25], poly(propylene glycol) (PPG) [26], poly(ethylene oxide) (PEO) [27], polymethyl methacrylate (PMMA) microspheres [28] and hexadecyl trimethyl ammonium bromide (CTAB) surfactant [18] in sol–gel route. However, pore sizes of porous TiO_2 films derived from pre-existing particles or molds are difficult to be precisely designed and regulated. Polymerization-induced phase separation is a

*Corresponding author. Tel./fax: +86 020 87112047.
E-mail address: cehhuang@scut.edu.cn (H. Huang).

0272-8842/$ - see front matter © 2013 Elsevier Ltd and Techna Group S.r.l. All rights reserved.
http://dx.doi.org/10.1016/j.ceramint.2013.06.087

template-free manufacturing method for porous structure in sol–gel process. In a typical phase separation process, chemical instability induced by polymerization triggers the formation of biphasic morphologies in the sol system, followed by an irreversible freezing of the transient morphology by the sol–gel transition of the gel phase. Upon removal of the non-gel phase, the gel phase becomes the porous skeleton, an oxide framework comprising of controlled macropores can be obtained [29,30]. It can be logically deduced that the degree of polymerization and the volume ratio of non-gel phase to gel phase can be controlled by adjusting polymerization rate or polymerization time. Consequently, pore size tailoring of oxide framework can be achieved successfully. However, effects of polymerization-induced phase separation on microspore size of TiO_2 films under template-free conditions are few reported.

TiO_2/SiO_2 composite thin films have been extensively used as anti-reflection, protective and self-cleaning coatings depending on their particular chemical composition and micromorphology [14,15,31,32]. Therefore, the performance of these materials can be dramatically advanced by morphological control in a broad length scale. In our previous work [14], macroporous TiO_2/SiO_2 (TS) composite thin films were successfully prepared through a novel sol–gel process by introducing of acetylacetone (AcAc) and diethanolamine (DEA) into the system, which could reduce the rate of hydrolysis of metal alkoxides and control the rate of polycondensation reactions by adjusting the pH of the sols, respectively. In this work, a facile pore size tailoring in a long range under template-free condition was achieved by adjusting the starting compositions or controlling the aging time. And the chemical reaction and the phase separation mechanism in the sol–gel process were elaborated. Lots of benefits are expected not only from the porous structure in the surface but also this novel approach, simplifying the experiment process of pore forming control under template-free condition.

2. Experimental

2.1. Chemicals

For the preparation of TiO_2/SiO_2 composite sols, the following materials were used as received: tetrabutyl titanate ($Ti(OC_4H_9)_4$, $Ti(OBu)_4$, 98.5%), tetraethyl orthosilicate ($Si(OC_2H_5)_4$, TEOS, 99%), anhydrous ethanol (C_2H_5OH, 99.7%), nitric acid (HNO_3, 65–68%), acetylacetone ($CH_3COCH_2COCH_3$, AcAc, 98%), diethanolamine ($(HOCH_2CH_2)_2NH$, DEA, 99%), deionized water (H_2O).

2.2. Preparations of TiO_2/SiO_2 composite sols

In a typical synthesis protocol, due to the wide difference in hydrolysis rate between $Ti(OBu)_4$ and TEOS, the TiO_2/SiO_2 composite sols were prepared by evenly mixing the separately-produced SiO_2 sol and TiO_2 sol. Firstly, a SiO_2 sol was prepared by mixing 10 ml TEOS with C_2H_5OH, H_2O and HNO_3 and the relative molar ratio of each chemical in the precursor sol was $TEOS:C_2H_5OH:H_2O:HNO_3 = 1:25:3:0.3$. The resulting sol was aged for 48 h before use. Then a starting TiO_2 solution was prepared by mixing 10 ml $Ti(OBu)_4$ with C_2H_5OH, AcAc, DEA, H_2O and HNO_3 and the relative molar ratio of each chemical in the precursor sol was $Ti(OBu)_4$: $AcAc:DEA:C_2H_5OH:H_2O:HNO_3 = 1:0.65:0.65:35:20:0.5$ [14]. Six groups of TS composite sols were obtained by mixing the SiO_2 sol and the starting TiO_2 and then were aged in different time before spin coating. The SiO_2 content, defined as a molar fraction % of Si/(Si+Ti) varied from 0, 10, 20, 30 and 40 to 50. And different SiO_2 content resulted composite sols were named as TS0, TS1, TS2, TS3, TS4 and TS5, respectively.

2.3. Preparations of TiO_2/SiO_2 composite films

The following describes the preparation of the porous TiO_2/SiO_2 composite films. Firstly, transparent glass substrates were carefully cleaned ultrasonically in acetone, C_2H_5OH and deionized water for 20 min, successively. Subsequently, the

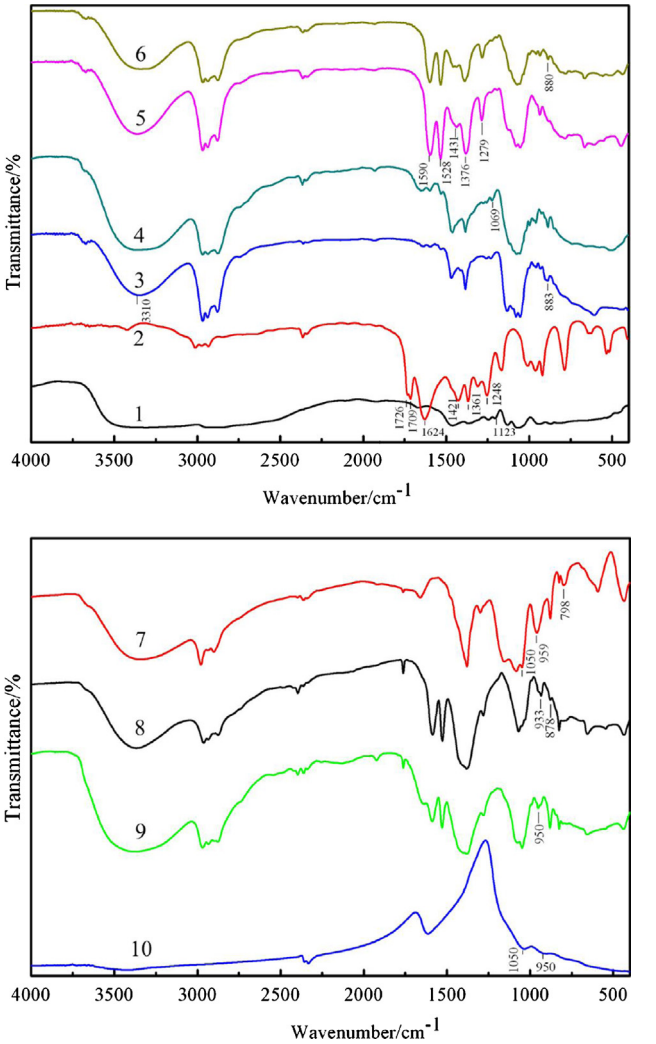

Fig. 1. FTIR spectra of TiO_2 sol–gel process: (1) DEA, (2) AcAc, (3) $Ti(OBu)_4+C_2H_5OH$, (4) $Ti(OBu)_4+C_2H_5OH$+DEA, (5) $Ti(OBu)_4+C_2H_5OH$ +AcAc, (6) $Ti(OBu)_4+C_2H_5OH$+AcAc+DEA, (7) SiO_2 sol, (8) TiO_2 sol, (9) TiO_2/SiO_2 composite sol (20%), and (10) TiO_2/SiO_2 composite powder (20%).

washed and dried substrates were spin-coated by the uniformly mixed precursor sols with the rotation speed of 800 rpm for 20 s and 3000 rpm for 30 s in succession. Finally, The coatings were dried at 100 °C for 0.5 h and then calcined in air at 500 °C for 1 h, at a heating rate of 5 °C/min.

2.4. Characterizations

The μm-range surface morphologies of TS composite films were measured by an LEO 1530 VP field emission scanning electrons microscope (FESEM). Fourier transform-infrared (FTIR) spectra of the composite TS sols and powders dispersed in KBr pellets were recorded on a Bruker Vector 33 spectrometer with a 6 cm^{-1} resolution in the frequency range from 4000 cm^{-1} to 400 cm^{-1}.

3. Results and discussion

3.1. Chemistry of the sol–gel process

3.1.1. Chemistry of TiO_2 sol

In a typical synthesis of the TiO_2 sol, the complexing agents AcAc and DEA have been reported as significant additives for controlling the rate of hydrolysis and precipitation of the metal alkoxides [18]. The related chemical reactions taking place are presumed as follows:

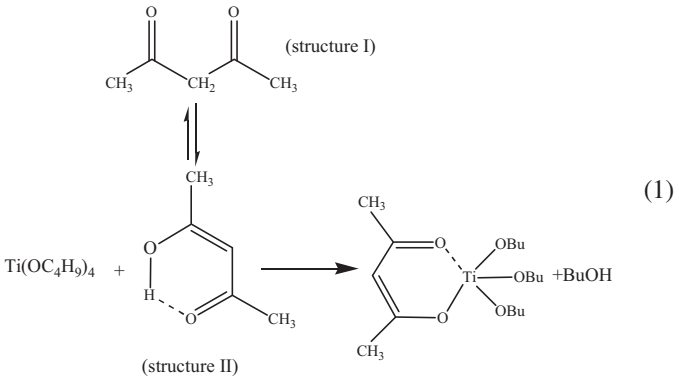

(1)

(2)

The chemical interactions between complexing agents and precursors in sol–gel progress could be deduced by analyzing FTIR spectra of the specimens. The evolution of the infrared spectra for different samples is represented in Fig. 1. When AcAc is added individually, it can be seen in traces 2, 3 and 5 that great changes take place in $Ti(OBu)_4$ precursor. It is well known that AcAc exists in two tautomeric forms (shown in Eq. (1)), i.e. the diketone form (structure I) and the enol form (structure II). The enol form was demonstrated by the spectrum of trace 2, in which the intense band of H–O–H bending vibration at 1624 cm^{-1} indicates the strong intramolecular hydrogen bond, compared with the normal absorption of conjugated ketones at 1726 and 1709 cm^{-1}. In the spectrum of trace 5, the bands observed at 1590 cm^{-1} are assigned to C═O stretching vibration of AcAc, and the bands at 1528 cm^{-1} are attributed to C═C stretching vibration bands, and both of them are shifted to low frequencies than those of free AcAc. This can be attributed to the formation of conjugated dimeric Ti(IV)–AcAc, which possesses strong electron-attracting tendency. Furthermore, the complexation of AcAc with Ti $(OBu)_4$ are also demonstrated by the disappearance of H–O–H bending vibration band at 1624 cm^{-1}, the blue shift of C–C–C absorption peak from 1248 to 1279 cm^{-1}, as well as the blue shift of $–CH_3$ bending vibration band peak from 1421, 1361 cm^{-1} to 1431 and 1376 cm^{-1}. On the other hand, when DEA is added only, as shown in traces 1, 4, the intensity of the N–H stretching vibration (about 3310 cm^{-1}) decreased and the C–N stretching vibration has a red shift from 1123 to 1069, indicating the complexation of DEA with $Ti(OBu)_4$. When both AcAc and DEA were used as complexing agents, as shown in trace 6, the main absorption peaks are almost the same as ones in trace 5, however, the characteristic absorption spectra of DEA has not changed obviously in the process, indicating that AcAc displays stronger chelating ability with $Ti(OBu)_4$ than DEA, together with $Ti(OBu)_4$ is considered to be complexed by AcAc only.

When H_2O is introduced into this system, the enol form of AcAc can react with $Ti(OBu)_4$ preferentially relative to the hydroxy in H_2O, which restrains the hydrolysis and condensation of $Ti(OBu)_4$ precursor, so as to maintain the stability of TiO_2 sol. Then the placid hydrolysis and polycondensation reactions of $Ti(OBu)_4$ precursor complexed by AcAc can be written as below:

1) Hydrolysis of $Ti(OBu)_4$ (single-molecule hydrolysis resultant as an example)

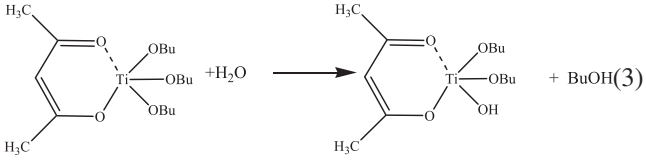

(3)

2) Dehydration and debutaniation polycondensation

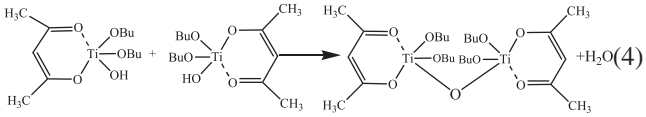

(4)

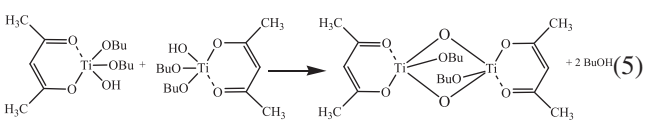

(5)

The hydrolysis reaction results in the formation of Ti $(OBu)_{4-x-y}(acac)_x(OH)_y$ with relatively strong polar, because of the contribution of hydroxyl group on the sol particle

Table 1
pH (after 2 days aging) and gel time of TS composite sols.

Sample	TS0	TS1	TS2	TS3	TS4	TS5
pH	5.85	5.18	4.11	2.98	1.66	1.50
Gel time/days	65	42	24	15	8	5

surface. Further dehydration and debutanation between the hydroxyl or alkoxy groups of $Ti(OBu)_{4-x-y}(acac)_x(OH)_y$ molecules lead to the condensation reactions. Therefore, relatively narrow distribution of growing titania oligomers can be obtained spontaneously in this condition [33]. This hydrolysis and condensation process can be demonstrated by curves 1, 6 and 8 as follow: (1) titanol groups characteristic peak (933 cm^{-1}) appear in the TiO_2 sol; (2) the characteristic peak of Ti–O–C_4H_9 gradually shifted toward lower frequency (883–878 cm^{-1}) together with decreasing the intensity, indicating the weakening or even destroying of the Ti–O–C_4H_9 chemical bonding.

3.1.2. Chemistry of SiO_2 sol

The hydrolysis and polycondensation reactions of TEOS precursor under acidic condition have been extensively studied by Houmard etc. [34]. In the presence of H_2O and HNO_3, the TEOS precursor is partially hydrolyzed to generate $Si(C_2H_5O)_3OH$. And then the hydrolysates can react with each other by polycondensation to form Si–O–Si bridging bonds. The above reactions can be confirmed by the IR spectrum of SiO_2 sol, which is shown in Fig. 1 (trace 7). The absorption peak at 1050 cm^{-1} is attributed to symmetric Si–O–Si stretching vibration and the IR absorbance at 798 cm^{-1} can be assigned to asymmetric Si–O–Si stretching vibration. The normalized spectra depict an IR band at 959 cm^{-1}, which is the characteristic of un-reacted silanol (Si–OH) group.

3.1.3. Chemistry of composite sols

According to the electrical double layer theory [35,36] and the aggregation of colloidal particles [37], in the pH range of our reaction conditions (about 1.5–6.0), the SiO_2 sol usually has negative zeta-potential, while the TiO_2 sol has positive zeta-potential. Therefore, when adding SiO_2 sol to TiO_2 sol, the SiO_2-polycondensate would attract titania oligomers and further react with them to generate a titania–silica condensation polymer. The composite process can be written as below

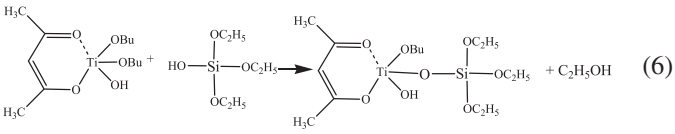

(6)

In trace 9 of FTIR spectra, an intense Ti–O–Si absorption peak at about 950 cm^{-1} appears, which indicates the forming of Ti–O–Si bond during the mixing process [38]. As the peak at 950 cm^{-1} in sols can be affected by the bands of silanol and titanol groups, in order to eliminate the influence of silanol and titanol groups, the IR spectrum of TiO_2/SiO_2 composite powders was recorded. The absorption peak appears at about 950 cm^{-1} in trace 10, which is a further evidence for the forming of Ti–O–Si bond and the occurring of the composite reaction.

3.2. The stability of TS sols

The pH values of TS composite sols were measured after 2 days of aging. As shown in Table 1, since the TiO_2 sol shows weak acidity, whereas the SiO_2 sol is highly acidic and its pH was less than 1, the pH values of mixing sols decreased gradually with the increased content of SiO_2 sol. The gel time was defined as the time period between the start point when TiO_2 and SiO_2 sols were mixed together and the end point when the composite sols become gelation and lost the ability to flow. As displayed in Table 1, the gel time of TS composite sols shortened dramatically with the increasing of SiO_2 sol content. In the process of above reactions (Eqs. (1)–(6)), the titania–silica oligomers in the composite sols coarsen gradually and then cross-link with each other. The resulting polycondensates bring about the increase in the viscosity and density of the composite sols, inducing the decrease of fluidity in sols as well as the emergence of gels. The more SiO_2 sol is added, the more complete reaction between titania oligomers and silica oligomers is obtained.

3.3. The phase separation in TiO_2 sol

Previous research has shown that a flat surface could be prepared through utilizing only AcAc or DEA as a complexing agent [39–41]. The situation, however, has thoroughly changed when both AcAc and DEA were used as complexing agents in this work. As shown in Fig. 4, a macroporous structure on TS0 surface was fabricated in a template-free sol–gel process, which can be attributed to the polymerization-induced phase separation in the TiO_2 sol. The mechanism and formation process of the phase separation was elaborated originating from a sol–gel system containing metal alkoxides and appropriate additives [29,42–44].

In this work, HNO_3 as the strong acid catalyst plays an important role of controlling the reactivity of $Ti(OBu)_4$ to H_2O. In acid conditions, the alkoxide of titanium exhibits much higher reactivity toward hydrolysis but relatively lower reactivity toward polycondensation. The key point is the use of AcAc and DEA as the complex agents. With the slow dropping of a mixture that consists of C_2H_5OH, H_2O and HNO_3, AcAc and DEA play two different, but equally important roles respectively. Since the complexing ability of AcAc is stronger than that of DEA, AcAc chelate with the alkoxides preferentially and therefore reduces the rate of hydrolysis and precipitation of metal alkoxides. Comparatively, DEA is a highly polar organic alkali solvent with hydrogen

bonding, when HNO_3 was introduced in the system, the H^+ would be consumed immediately by neutralization in a small region. The pH in this small region decreases spontaneously to isoelectric point of TiO_2 (pH=5.5–6.0) [30]. Even though the regional pH influenced by the nearby OH^- will increase in a short time, the rapid change of pH to neutral condition accelerates the polycondensation reaction in this short moment. Debutanation polycondensation and dehydration polycondensation gradually decrease the polarity of titania oligomers by consuming the hydroxyl groups, whereas the polarity of the solvent remains high. In the course of polycondensation, therefore, the initially homogeneous mixture was destroyed, resulting from the reduction of miscibility between the polar solvent and polycondensed inorganic species. This mechanism of the original phase separation is described in Fig. 2, through adjusting the pH to neutral condition, phase separation will be triggered by accelerating polycondensation reaction which leads to the polarity gap of solvent and solute phases. Satisfactory regional pH can be obtained from pre-setting mother solution pH and regional neutralization.

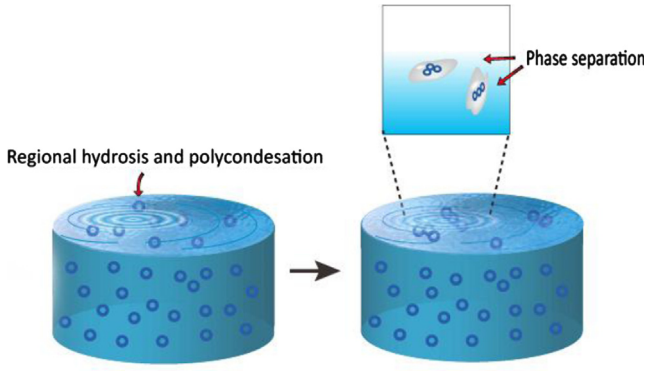

Fig. 2. Schematic diagram of the original phase separation in TiO_2 system.

When the solution is deposited on the surface of glass substrate by spin-coating, the developing phase-separating

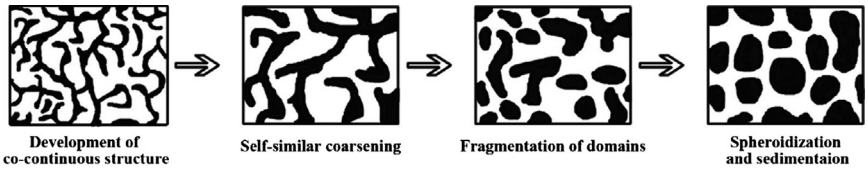

Fig. 3. The schematic illustration of developing phase separation in and spinodal decomposition.

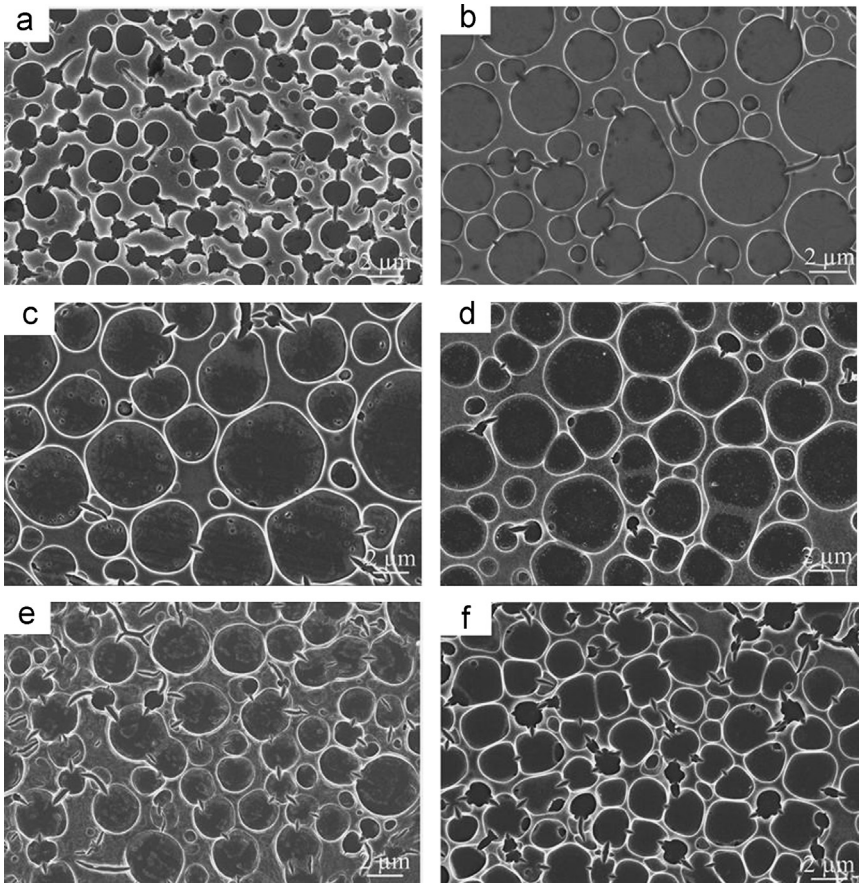

Fig. 4. SEM micrographs of TiO_2 thin films at different aging times, (a) 0 day, (b) 1 day, (c) 2 days, (d) 5 days, (e) 10 days and (f) 15 days.

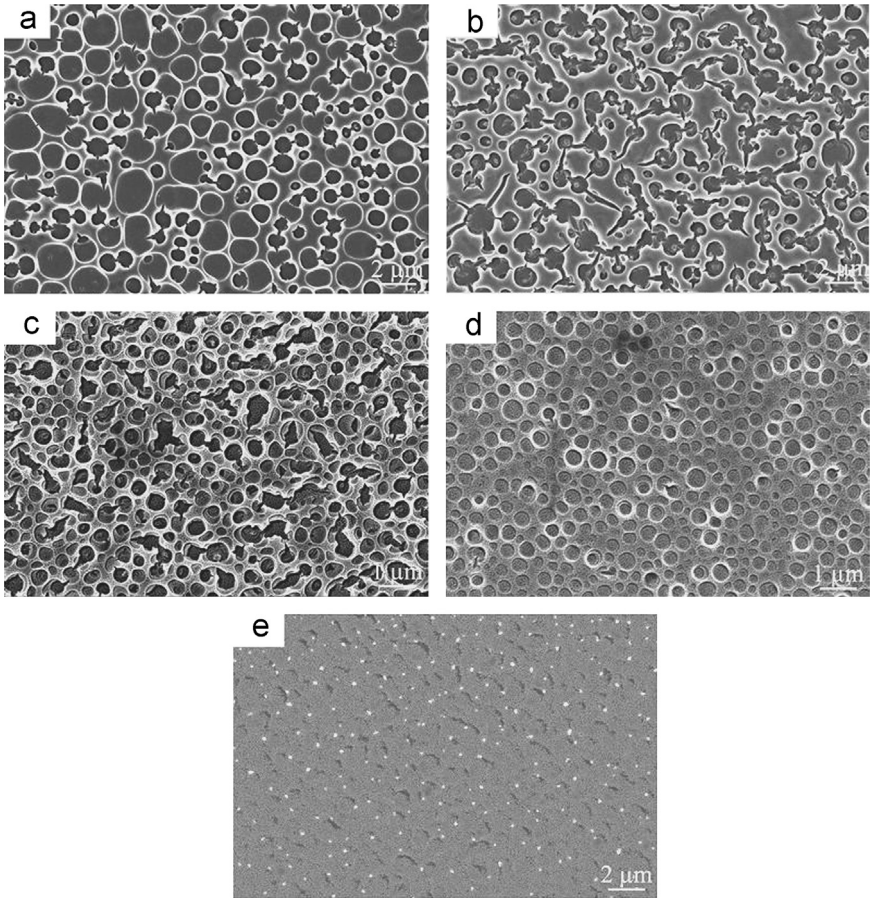

Fig. 5. SEM micrographs of TS composite thin films after 2 days of aging at different mol contents of SiO_2: (a) 10%, (b) 20%, (c) 30%, (d) 40% and (e) 50%.

domains are solidified suddenly by an evaporation-induced sol–gel transition. Two-dimensionally phase-separated structures on the substrate are formed by the rapid physical freezing of the transient structure. The domains of solvent phase are expelled from the substrate to form unoccupied regions, while the domains of gel phase tend to spread on the substrate and form porous skeleton porous skeleton. Since the sol–gel transition occurs simultaneously with the structural development of the phase separation, the transient structures can be frozen in various stages. Therefore, various transient structures can be obtained as a permanent gel morphology between the onset of phase separation and gel formation. The porous structures depend on the competitive relation of phase separation and sol–gel transition, therefore, are controlled by the onset of phase separation relative to the sol–gel transition point. The earlier the phase separation is initiated relative to the sol–gel transition, the coarser the resultant structure becomes, and vice versa. In order to confirm the mechanisms of the phase separation and investigate the adjusting method for porous structure size of the TiO_2 film, the change process of porous structure under different aging times were studied.

For the TiO_2 sol with the complexing agents of AcAc and DEA, the sol–gel transition is very slow and the sol has a long stable time, which is very helpful for the formation of stable porous structures. Seen from Fig. 4, with the aging times from 0 day to 15 days, extraordinarily formed and stable interconnected or isolated pores appeares in TiO_2 surface. The average pore size of the films increases from 1 to 3.5 μm in the initial stage (0–2 days aging time) with the development of spinodal decomposition, and the schematic illustration of developing phase separation in spinodal decomposition is described in Figs. 3 and 4. However, when the aging time continually increases, the gelling tendency of TiO_2 sol is strengthened and the TiO_2 gel phase formed in the polycondensation may be satisfactorily crosslinked though consuming or absorbing the solvent, leading to an increasing compatibility of the two phases and the gradual collapse of macropores. For this reason, the phase separation is restrained and the average size of the porous films decreased from about 3.5 to 2 μm (2–15 days aging time). Therefore, the aging time is an important influence factor for phase separation, and a relatively precise pore size adjustment can be obtained by changing the aging time.

3.4. Effect of the amount of SiO_2 sol

For investigating the influence of the SiO_2 sol on the morphology of TS thin films, the TS composite thin films with different amounts of SiO_2 after the same 2 days of aging time are operated. Seen from Fig. 5, the addition amount ratio of SiO_2 to TiO_2 sol significantly affected the phase separation degree and

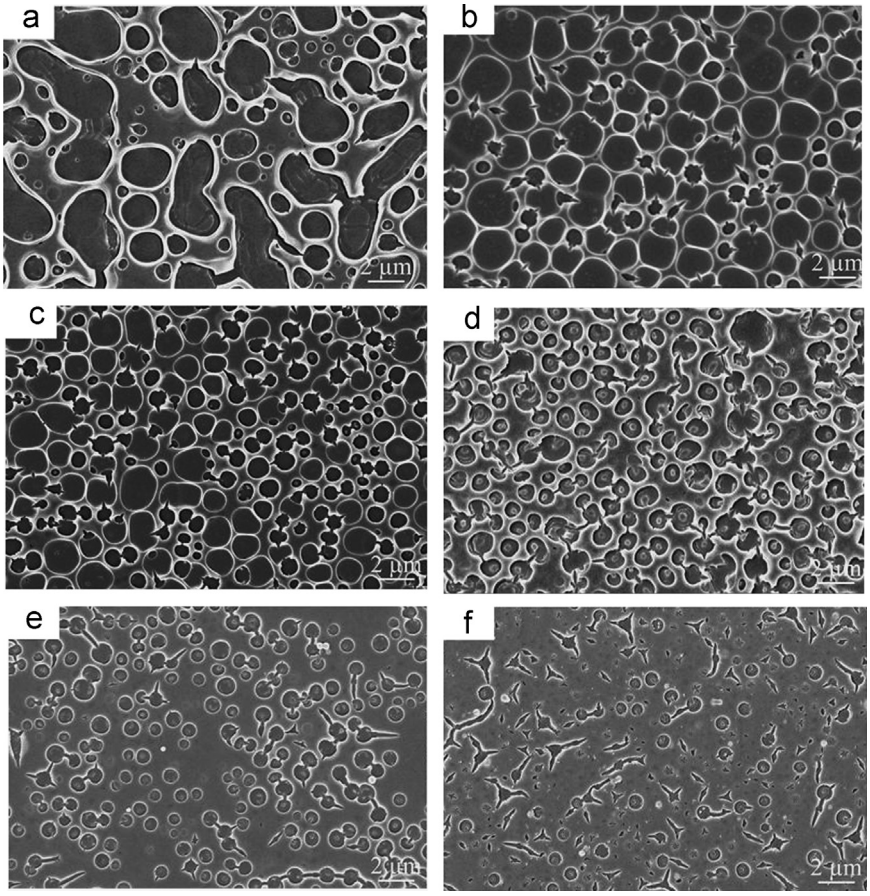

Fig. 6. SEM micrographs of TS composite thin films with 10% SiO_2 at different aging times, (a)–(g) represent 0–5 days, correspondingly.

surface morphology of TS composite thin films. In the diagrams, interconnected or isolated macropores in TS1, TS2, TS3, and TS4 surfaces turned to shrink with gradual increasing of SiO_2 content from 10% to 40%, exhibiting numerous macropores with average size around 1.5 μm, 1.2 μm, 500 nm and 400 nm, respectively. Moreover, when the SiO_2 content further increased to 50%, the porous structure has almost disappeared, and only some slight traces of porous skeleton can be found.

There would be three main reasons for the gradually suppressed phase separation in the TiO_2 sol by the introduction of SiO_2 sol. Firstly, when SiO_2 sol (with non-phase-separation) was added, it acts as a co-solvent of the relatively incompatible titania oligomers in the reaction solution [45]. So the phase separation tendency was suppressed due to the dilution effect, leading to smaller phase separation domains in the whole TiO_2/SiO_2 sol system. Hence, the more SiO_2 sol added, the smaller porous structure obtained. Secondly, pH act as a significant factor in the TiO_2 sol for the control of polycondensation rate [29,30]. The pH of each component solution system is given in Table 1. The organic alkali DEA could be consumed by the excessive HNO_3 in SiO_2 sol, and the final pH ultimately decreased to 1.50. Since the solution pH of TS3, TS4 and TS5 sol are about 2.98, 1.66 and 1.50, which are much lower than the isoelectric point of TiO_2 [30], the alkoxy-derived oligomers are positively charged and spontaneously stabilized by the electrostatic repulsion. They grow into broader distribution by successive condensation, which slow down the onset of phase separation relative to the sol–gel transition point and being an obstacle to phase separation. Finally, as the gel time decrease dramatically from TS0 to TS5, so in the same 2 days aging times, the gelling tendency of TS sol is strengthened obviously from TS0 to TS5. As the previous analysis, the compatibility of the solvent-rich and oligomer-rich phases increases in this system.

3.5. Effect of aging times

Fig. 6 shows the FESEM images of TS1 thin films with different aging times. A lot of co-continuous structure contains negative or positive curvature surfaces, as well as some porous structure can be clearly observed in Fig. 6a. It can be obviously observed that the phase separation in TiO_2/SiO_2 sol system is dominated by the "spinodal decomposition" mechanisms, and the state of phase-separation domains in TS1 sol without aging period is full of the co-continuous and fragmented structure. After 1 day aging time, the fragmentation and spheroidization of the phase-separation domains has become the main state, and the obtained macroporous structure has a pore size of approximately 2 μm. From Fig. 6a and b, we can see an integrated spinodal decomposition regulated phase-separation process.

However, when the aging is sustaining to five days, the pore size became smaller from 2 μm to 400 nm and the amount of pore became fewer. And the similar phenomena happen in the

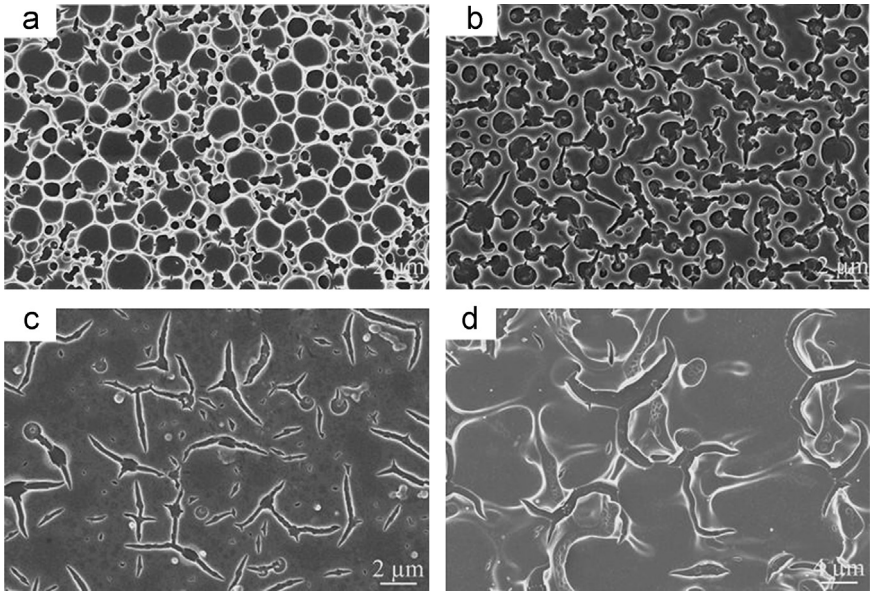

Fig. 7. SEM micrographs of TS2 thin films prepared after different aging times: (a) 1 day, (b) 2 days, (c) 3 days and (d) 4 days.

TS2 films, in which the pore size gradually become smaller until it disappear (see in Fig. 7). We can conclude that the phase separation of the TS sol is gradually suppressed by increasing aging time. One interpretation of the phenomenon is that the dilution effect by introduced SiO_2 sol is a continuous, but slow process, and the phase separation tendency is suppressed accompanied by decreased hydrolysis–polycondensation reaction rate [45]. Another tentative inference on this result is that phase separation tendency is restrained by the ever-increasing gelling tendency of TiO_2 sol. This deduction can be supported by the SEM micrographs of TS0, TS1 and TS2 films obtained by the different aging times. From TS0 to TS2, the rate of gelling tendency accelerates, so the phase separation tendency is suppressed more quickly, that is to say, the pore size decreases more faster.

In brief, by inducing a phase separation parallel to the sol–gel transition of alkoxy-derived TiO_2 or TiO_2–SiO_2 system, films with well-defined macroporous structure can be prepared. With an appropriate choice of the reaction conditions such as starting composition and aging time, the pore size of composite films can be designed in a broad range. When both the effects of the amount of SiO_2 sol and aging times are taken into consideration, the pore size of the TS films can be tailored in a long range (about 100 nm–2 μm) by adjusting the starting compositions or controlling the aging time. In view of the stability and homogeneity of the macroporous morphology, together with the competitive relation of phase separation and sol–gel transformation, the optimum approach to construct TS films would be design the starting composition of 10% content SiO_2 and controlling the aging time of 1–2 days.

4. Conclusions

TiO_2/SiO_2 composite thin films with macroporous structure have been prepared by a sol–gel process in template-free conditions. The macroporous morphology is obtained by polymerization-induced phase separation and the concurrent sol–gel transition process. The phase separation mechanism of the sol system is proved to be the spinodal decomposition. The porous structure of TS is influenced significantly by the amount of SiO_2 and aging time. With increasing SiO_2 content or extending aging time, the pore size became smaller since the phase separation was suppressed gradually in the composite sol. The diameter of macropores on the TS composite thin films could be tailored in a long range by adjusting the starting compositions or controlling the aging time, which facilitates the application of TiO_2/SiO_2 composite thin films in various fields.

Acknowledgments

The authors gratefully thank the National Nature Science Foundation of China (51103045) and the Fundamental Research Funds for the Central University, SCUT (2012ZM0036) for financial support of this work.

References

[1] A. Fujishima, K. Honda, Electrochemical photolysis of water at a semiconductor electrode, Nature 238 (1972) 37–38.
[2] R. Wang, K. Hashimoto, A. Fujishima, M. Chikuni, E. Kojima, A. Kitamura, M. Shimohigoshi, T. Watanabe, Light-induced amphiphilic surfaces, Nature 388 (1997) 431–432.
[3] M. Arin, P. Lommens, N. Avci, S.C. Hopkins, K. De Buysser, I.M. Arabatzis, I. Fasaki, D. Poelman, I. Van Driessche, Inkjet printing of photocatalytically active TiO_2 thin films from water based precursor solutions, Journal of the European Ceramic Society 31 (2011) 1067–1074.
[4] Y.-F. Zhu, J. Zhang, Y.-Y. Zhang, M. Ding, H.-Q. Qi, R.-G. Du, C.-J. Lin, Anticorrosion properties of modified nano-TiO_2 films prepared by sol–gel method, Acta Physico Chimica Sinica 28 (2012) 393–398.
[5] G. Dai, L. Zhao, J. Li, L. Wan, F. Hu, Z. Xu, B. Dong, H. Lu, S. Wang, J. Yu, A novel photoanode architecture of dye-sensitized solar cells based on TiO_2 hollow sphere/nanorod array double-layer film, Journal of Colloid and Interface Science 365 (2012) 46–52.
[6] T.-J. Ha, S.-Y. Jung, J.-H. Bae, H.-L. Lee, H.W. Jang, S.-J. Yoon, S. Shin, H.H. Cho, H.-H. Park, Analysis of heat transfer in ordered and

disordered mesoporous TiO_2 films by finite element analysis, Microporous and Mesoporous Materials 144 (2011) 191–194.
[7] F. Rupp, M. Haupt, H. Klostermann, H.S. Kim, M. Eichler, A. Peetsch, L. Scheideler, C. Doering, C. Oehr, H.P. Wendel, S. Sinn, E. Decker, C. von Ohle, J. Geis-Gerstorfer, Multifunctional nature of UV-irradiated nanocrystalline anatase thin films for biomedical applications, Acta Biomaterialia 6 (2010) 4566–4577.
[8] D. Tahk, T.-I. Kim, H. Yoon, M. Choi, K. Shin, K.Y. Suh, Fabrication of antireflection and antifogging polymer sheet by partial photopolymerization and dry etching, Langmuir 26 (2010) 2240–2243.
[9] F.R. Marciano, D.A. Lima-Oliveira, N.S. Da-Silva, A.V. Diniz, E.J. Corat, V.J. Trava-Airoldi, Antibacterial activity of DLC films containing TiO_2 nanoparticles, Journal of Colloid and Interface Science 340 (2009) 87–92.
[10] D.P. Serrano, G. Calleja, R. Sanz, P. Pizarro, Development of crystallinity and photocatalytic properties in porous TiO_2 by mild acid treatment, Journal of Materials Chemistry 17 (2007) 1178–1187.
[11] B. Peng, L. Tan, D. Chen, X. Meng, F. Tang, Programming surface morphology of TiO_2 hollow spheres and their superhydrophilic films, ACS Applied Materials and Interfaces 4 (2011) 96–101.
[12] Y. Yao, N. Zhao, J.-J. Feng, M.-M. Yao, F. Li, Photocatalytic activities of Ce or Co doped nanocrystalline $TiO_2 \cdot SiO_2$ composite films, Ceramics International 39 (2013) 4735–4738.
[13] K. Laohhasurayotin, S. Pookboonmee, D. Viboonratanasri, W. Kangwansupamonkon, Preparation of magnetic photocatalyst nanoparticles-TiO_2/SiO_2/Mn–Zn ferrite and its photocatalytic activity influenced by silica interlayer, Materials Research Bulletin 47 (2012) 1500–1507.
[14] T. Huang, W. Huang, C. Zhou, Y. Situ, H. Huang, Superhydrophilicity of TiO_2/SiO_2 thin films: synergistic effect of SiO_2 and phase-separation-induced porous structure, Surface and Coatings Technology 213 (2012) 126–132.
[15] Y.Y. Liu, L.Q. Qian, C. Guo, X. Jia, J.W. Wang, W.H. Tang, Natural superhydrophilic TiO_2/SiO_2 composite thin films deposited by radio frequency magnetron sputtering, Journal of Alloys and Compounds 479 (2009) 532–535.
[16] S. Permpoon, M. Houmard, D. Riassetto, L. Rapenne, G. Berthome, B. Baroux, J.C. Joud, M. Langlet, Natural and persistent superhydrophilicity of SiO_2/TiO_2 and TiO_2/SiO_2 bi-layer films, Thin Solid Films 516 (2008) 957–966.
[17] J.J. Wang, D.S. Wang, J.A. Wang, W.L. Zhao, C.W. Wang, High transmittance and superhydrophilicity of porous TiO_2/SiO_2 bi-layer films without UV irradiation, Surface and Coatings Technology 205 (2011) 3596–3599.
[18] G. Liu, Z. Jin, X. Liu, T. Wang, Z. Liu, Anatase TiO_2 porous thin films prepared by sol-gel method using CTAB surfactant, Journal of Sol–Gel Science and Technology 41 (2007) 49–55.
[19] M. Horprathum, P. Chindaudom, P. Limnonthakul, P. Eiamchai, N. Nuntawong, V. Patthanasettakul, A. Pokaipisit, P. Limsuwan, Fabrication and characterization of hydrophilic TiO_2 thin films on unheated substrates prepared by pulsed DC reactive magnetron sputtering, Journal of Nanomaterials 2010 (2010) Article ID 841659, 7 pp. http://dx.doi.org/10.1155/2010/841659.
[20] C.S. Kuo, Y.H. Tseng, Y.Y. Li, Wettability and superhydrophilic TiO_2 film formed by chemical vapor deposition, Chemistry Letters 35 (2006) 356–357.
[21] D. Hanaor, M. Michelazzi, J. Chenu, C. Leonelli, C.C. Sorrell, The effects of firing conditions on the properties of electrophoretically deposited titanium dioxide films on graphite substrates, Journal of the European Ceramic Society 31 (2011) 2877–2885.
[22] D. Li, J. Zhang, L. Shao, C. Chen, G. Liu, Y. Yang, Preparation and photocatalytic properties of nanometer TiO_2 thin films by improved ultrasonic spray pyrolysis, Rare Metals 30 (2011) 233–237.
[23] E. Hosono, H. Matsuda, I. Honma, M. Ichihara, H. Zhou, Synthesis of a perpendicular TiO_2 nanosheet film with the superhydrophilic property without UV irradiation, Langmuir 23 (2007) 7447–7450.
[24] A. Dutschke, C. Diegelmann, P. Lobmann, Preparation of TiO_2 thin films on polystyrene by liquid phase deposition, Journal of Materials Chemistry 13 (2003) 1058–1063.
[25] S.-H. Wang, K.-H. Wang, Y.-M. Dai, J.-M. Jehng, Water effect on the surface morphology of TiO_2 thin film modified by polyethylene glycol, Applied Surface Science 264 (2013) 470–475.
[26] L. Malfatti, M.N.G. Bellino, P. Innocenzi, G.J.A.A. Soler-Illia, One-pot route to produce hierarchically porous titania thin films by controlled self-assembly, swelling, and phase separation, Chemistry of Materials 21 (2009) 2763–2769.
[27] Q.L. Wu, N. Subramanian, S.E. Rankin, Hierarchically porous titania thin film prepared by controlled phase separation and surfactant templating, Langmuir 27 (2011) 9557–9566.
[28] H. Zhang, F. Dong, S. Fang, C. Ye, M. Wang, H. Cheng, Z. Han, S. Zhai, Fabrication of macroporous titanium dioxide film using PMMA microspheres as template, Journal of Colloid and Interface Science 386 (2012) 73–79.
[29] J. Konishi, K. Fujita, K. Nakanishi, K. Hirao, Monolithic TiO_2 with controlled multiscale porosity via a template-free sol−gel process accompanied by phase separation, Chemistry of Materials 18 (2006) 6069–6074.
[30] K. Nakanishi, N. Tanaka, Sol–gel with phase separation. hierarchically porous materials optimized for high-performance liquid chromatography separations, Accounts of Chemical Research 40 (2007) 863–873.
[31] M. Hirano, K. Ota, Direct formation and photocatalytic performance of anatase (TiO_2)/silica (SiO_2) composite nanoparticles, Journal of the American Ceramic Society 87 (2004) 1567–1570.
[32] A. Tricoli, M. Righettoni, S.E. Pratsinis, Anti-fogging nanofibrous SiO_2 and nanostructured SiO_2–TiO_2 films bade by rapid flame deposition and in situ annealing, Langmuir 25 (2009) 12578–12584.
[33] S.J. Bu, Z.G. Jin, X.X. Liu, L.R. Yang, Z.J. Cheng, Synthesis of TiO_2 porous thin films by polyethylene glycol templating and chemistry of the process, Journal of the European Ceramic Society 25 (2005) 673–679.
[34] M. Houmard, D. Riassetto, F. Roussel, A. Bourgeois, G. Berthomé, J.C. Joud, M. Langlet, Morphology and natural wettability properties of sol–gel derived TiO_2–SiO_2 composite thin films, Applied Surface Science 254 (2007) 1405–1414.
[35] A. Teleki, M.K. Akhtar, S.E. Pratsinis, The quality of SiO_2-coatings on flame-made TiO_2-based nanoparticles, Journal of Materials Chemistry 18 (2008) 3547–3555.
[36] M. Zhang, L. Shi, S. Yuan, Y. Zhao, J. Fang, Synthesis and photocatalytic properties of highly stable and neutral TiO_2/SiO_2 hydrosol, Journal of Colloid and Interface Science 330 (2009) 113–118.
[37] M. Kobayashi, F. Juillerat, P. Galletto, P. Bowen, M. Borkovec, Aggregation and charging of colloidal silica particles: effect of particle size, Langmuir 21 (2005) 5761–5769.
[38] Y.Farhang Ghoje Biglu, E. Taheri-Nassaj, Investigation of phase separation of nano-crystalline anatase from TiO_2SiO_2 thin film, Ceramics International 39 (2012) 2511–2518.
[39] W.X. Huang, H. Huang, H. Li, Z.H. Zhou, H. Chen, Superhydrophilic nano-TiO_2 film with porous surface structure, Materials Research Innovations 13 (2009) 459–463.
[40] W.X. Huang, W. Deng, M. Lei, H. Huang, Superhydrophilic porous TiO_2 film prepared by phase separation through two stabilizers, Applied Surface Science 257 (2011) 4774–4780.
[41] W.X. Huang, M. Lei, H. Huang, J.C. Chen, H.Q. Chen, Effect of polyethylene glycol on hydrophilic TiO_2 films: porosity-driven superhydrophilicity, Surface and Coatings Technology 204 (2010) 3954–3961.
[42] J. Konishi, K. Fujita, K. Nakanishi, K. Hirao, K. Morisato, S. Miyazaki, M. Ohira, Sol–gel synthesis of macro-mesoporous titania monoliths and their applications to chromatographic separation media for organophosphate compounds, Journal of Chromatography A 1216 (2009) 7375–7383.
[43] B. Gaweł, K. Gaweł, G. Øye, Sol–gel synthesis of non-silica monolithic materials, Materials 3 (2010) 2815–2833.
[44] G. Hasegawa, K. Kanamori, K. Nakanishi, T. Hanada, Facile preparation of hierarchically porous TiO_2 monoliths, Journal of the American Ceramic Society 93 (2010) 3110–3115.
[45] K. Nakanishi, Sol–gel process of oxides accompanied by phase separation, Bulletin of the Chemical Society of Japan 79 (2006) 673–691.